Nonlinear stochastic resonance: The saga of anomalous output-input gain

Peter Hänggi,[1,2] Mario E. Inchiosa,[2] Dave Fogliatti,[2] and Adi R. Bulsara[2]
[1]*Institut für Physik, Universität Augsburg, Universitätstrasse 1, D-86135 Augsburg, Germany*
[2]*SPAWAR Systems Center San Diego, Code D364, San Diego, California 92152-5001*
(Received 18 May 2000)

We reconsider stochastic resonance (SR) for an overdamped bistable dynamics driven by a harmonic force and Gaussian noise from the viewpoint of the gain behavior, i.e., the signal-to-noise ratio (SNR) at the output divided by that at the input. The primary issue addressed in this work is whether a gain exceeding unity can occur for this archetypal SR model, for subthreshold signals that are beyond the regime of validity of linear response theory: in contrast to nondynamical threshold systems, we find that the nonlinear gain in this conventional SR system exceeds unity only for suprathreshold signals, where SR for the spectral amplification and/or the SNR no longer occurs. Moreover, the gain assumes, at weak to moderate noise strengths, rather small (minimal) values for near-threshold signal amplitudes. The SNR gain generically exhibits a distinctive nonmonotonic behavior versus both the signal amplitude at fixed noise intensity and the noise intensity at fixed signal amplitude. We also test the validity of linear response theory; this approximation is strongly violated for weak noise. At strong noise, however, its validity regime extends well into the large driving regime above threshold. The prominent role of physically realistic noise color is studied for exponentially correlated Gaussian noise of constant intensity scaling and also for constant variance scaling; the latter produces a characteristic, resonancelike gain behavior. The gain for this typical SR setup is further contrasted with the gain behavior for a ''soft'' potential model.

PACS number(s): 05.40.−a, 05.45.−a, 02.50.Ey, 02.60.Cb

I. INTRODUCTION

Stochastic resonance (SR) characterizes a cooperative phenomenon wherein the addition of a small amount of noise to an input driving signal can optimally amplify the output response. Generically the phenomenon occurs in nonlinear stochastic classical and quantum systems which possess a kind of metastability such as a potential barrier, a fixed threshold, or, more generally, a statistical distribution of level-crossing features. An introductory overview of this most challenging phenomenon can be found in Refs. [1,2] while a comprehensive survey is provided in Ref. [3]. As such, the SR effect plays a prominent role in such diverse scientific areas as sensory biology, signal information and detection, or in conventional physical and chemical nonlinear noisy systems that are externally perturbed by periodic or aperiodic forces. Given the three features of (i) nonlinearity, (ii) a weak information carrying signal, and (iii) a source of noise, the response of the system generically undergoes a nonmonotonic signal transduction behavior as a function of increasing noise intensity: the response typically displays one or sometimes more maxima as a function of noise intensity, hence the term ''stochastic resonance.'' Typical quantifiers for SR in the case of time-periodic input signals are the spectral power amplification (SPA) [4,5] and/or the signal-to-noise ratio (SNR) [6]. For more general inputs, such as nonstationary, stochastic, and wideband signals, the adequate SR quantifiers are information-theoretic measures [7] such as the mutual information, the information distance, or the rate of information gain, to name but a few [8]. For signal detection systems, the effect of SR on detection performance is quantified by signal detection statistics such as the probability of detection and probability of a false alarm, which are often plotted against each other to form a curve known as the receiver operating characteristic (ROC) [9].

Throughout this work we shall concentrate on conventional SR setups that are fed by a harmonic input signal $A_0 \cos(\Omega t+\phi)$. The main question to be addressed with this work is the saga that relates the behavior of the gain G, i.e.,

$$G=\frac{R_{\mathrm{out}}}{R_{\mathrm{in}}} \tag{1}$$

between the *output* R_{out} and the R_{in} to the strength of the signal input A_0 and the noise characteristics such as its intensity and its strength of color. For weak signals it follows from a straightforward application of linear response theory [5,6,10–12] that the gain cannot exceed unity [13].

Recently, there has been considerable interest in the response of threshold systems (or static nonlinearities), wherein the SR effect also occurs, but bears a very strong resemblance to ''dither,'' a connection that was recently quantified by Gammaitoni [14]. In contrast to dynamical systems, for SR occurring in these *nondynamical* threshold systems such as in a level-crossing detector [15] or SR in the generalized two-threshold system as characterized by a static nonlinearity [16], which are all driven by periodic, rectangular-shaped pulses $s(t)$ of short duration, it has been demonstrated [15,16] that the gain can indeed exceed unity for moderate to strong *subthreshold* pulses. For a smooth harmonic input passing through a soft limiter, given by a nonhysteretic rf superconducting quantum interference device (SQUID) loop, a gain exceeding unity has been observed as well [17]. Therefore, it seems likely that the gain can exceed unity at no risk if only the response is *beyond* the regime of vality of *linear response*. The challenge to be addressed with this work is to settle this very issue for the most conventional SR setup: namely, a harmonically driven, over-

damped dynamics in a symmetric double well. The regime of nonlinear response for this archetypal SR system has been addressed previously from the viewpoint of nonlinear spectral amplification, $R_{\rm out}$ [4,5] and the corresponding phase lag of the nonlinear response [18,19], its universal weak noise SR behavior [20–22], its switching and dynamic trapping behavior for suprathreshold and near-threshold driving strengths [23], or the control of SR [24] by the relative phase of a harmonic mixing signal [25]. Also, an SNR gain exceeding unity has been briefly studied for an overdamped particle in a ''soft'' (nonquartic) double-well neuron potential driven by a suprathreshold sine wave plus *bandpass-filtered* noise (see Fig. 11 in [26]); however, a detailed study of SNR gain behavior with delta- or exponentially correlated noise has not yet been put forward. Our objective here is to fill this very gap with a systematic study. In particular, we want to investigate whether a gain exceeding unity generically occurs in conventional SR setups for subthreshold signals that exhibit *nonlinear* SR, or whether it requires strong suprathreshold signals. Thereby, the role of linear response theory will be reinvestigated quantitatively as a function of increasing signal strength. Moreover, we will research the role of noise color for the gain behavior.

II. ARCHETYPAL MODEL FOR SR

We start by considering the most common SR situation, namely, an overdamped dynamics driven by white Gaussian noise in a symmetric, quartic bistable double well. In terms of rescaled variables (see [27] for details) the dimensionless driven dynamics obeys the Langevin equation

$$\dot{x} = x - x^3 + A_0 \cos(\Omega t + \phi) + \sqrt{2D}\,\xi(t), \tag{2}$$

with $\xi(t)$ being Gaussian white noise with correlation $\langle \xi(t)\xi(s)\rangle = \delta(t-s)$ and ϕ an arbitrary, fixed phase of the coherent drive. The deterministic driven dynamics in Eq. (2) loses its global bistable character when the driving strength A_0 exceeds the threshold value $A_0 \geqslant A_T := \sqrt{4/27} \approx 0.3849$.

This archetypal driven bistable dynamics generally yields a nonlinear response: its asymptotic time-periodic expectation reads in terms of the complex-valued spectral weights M_n [3,27]

$$\langle x(t)\rangle_{as} = \sum_{n=-\infty}^{\infty} M_n \exp[i\,n(\Omega t + \phi)]. \tag{3}$$

The correlation function of the driven stochastic process $x(t)$, averaged over *both* the noise $\xi(t)$ and the uniformly distributed phase ϕ, obeys, in the asymptotic long-time limit, the *time-homogenous* result

$$\langle\langle x(t+\tau)x(t)\rangle\rangle := K(\tau) = K_{\rm noise}(\tau) + K_{as}(\tau), \tag{4}$$

wherein the asymptotic part denotes the oscillatory long-time limit, i.e.,

$$K_{as}(\tau) = 2\sum_{n=1}^{\infty} |M_n|^2 \cos(n\Omega\tau). \tag{5}$$

The power spectral density (PSD) of the time-homogeneous correlation $K(\tau)$ is defined as

$$K(\omega) := \int_{-\infty}^{\infty} \exp(-i\omega\tau) K(\tau)\, d\tau. \tag{6}$$

Hence, the total integrated input power of the cosine drive accordingly is $2\pi(A_0^2/2) = \pi A_0^2$. The spectral amplification η [5] is then given by the ratio of the integrated power of the asymptotic power spectrum $K_{as}(\omega)$ of the two δ-function weights located at $\pm\Omega$ and the total input power, yielding

$$\eta = \frac{4\pi |M_1(A_0,\Omega)|^2}{\pi A_0^2} = \left(\frac{2|M_1(A_0,\Omega)|}{A_0}\right)^2. \tag{7}$$

The SNR's are defined as follows: In terms of the power spectrum of the output $x(t)$, i.e., $K_{\rm noise}(\omega=\Omega) := K_{\rm noise}(\Omega; A_0, D)$, and the power spectrum of the input noise $\Xi(\omega) = 2D$ we obtain for the output SNR

$$R_{\rm out} = \frac{4\pi |M_1(A_0,\Omega)|^2}{K_{\rm noise}(\Omega; A_0, D)}, \tag{8}$$

while the input SNR reads

$$R_{\rm in} = \frac{\pi A_0^2}{\Xi(\Omega)} = \frac{\pi A_0^2}{2D}. \tag{9}$$

The quantity of interest, namely, the SNR gain in Eq. (1), is thus given by the result

$$G = \frac{\Xi(\Omega) 4\pi |M_1(A_0,\Omega)|^2}{\pi A_0^2 K_{\rm noise}(\Omega; A_0, D)}, \tag{10}$$

which clearly does not exceed unity as the driving strength approaches zero (linear response limit). Because we consider mainly the nonlinear driving regime, these expressions are difficult to evaluate by analytical means. An analytical evaluation is possible for the adiabatic driving regime; its explicit evaluation requires, however, the need of numerics. Therefore, we stick to a full nonlinear numerical evaluation throughout the remaining parts of this paper. Some details of the numerical scheme are summarized in the Appendix.

III. GAIN FOR WHITE GAUSSIAN NOISE DRIVEN SR

We start our SNR gain comparison with the white noise driven overdamped dynamics in Eq. (2). In Fig. 1 we depict the power spectrum of the output noise background, i.e., $K_{\rm noise}(\omega)$ in Eq. (4), for a weak driving amplitude (linear response limit) $A_0 = 0.1A_T$ and a strong driving amplitude $A_0 = 10A_T$. We note that at frequencies near the driving frequency $\omega = \Omega = 0.1$ and below, the noise power spectral density undergoes a drastic reduction with increasing driving strength. This already suggests that the increase in SNR gain is mainly controlled by the behavior of the noise power spectrum, considering that the spectral amplification η exhibits a decreasing behavior versus increasing driving strength A_0 [3,5].

For subthreshold driving, probing the double well at very

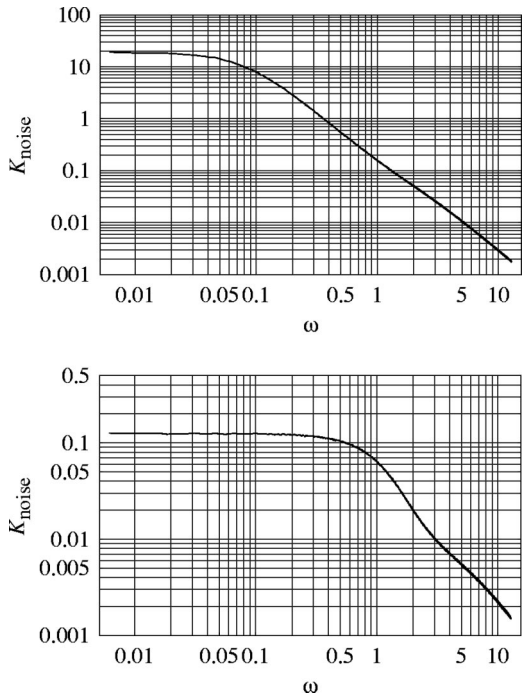

FIG. 1. The output noise power spectrum $K_{\text{noise}}(\omega)$, for weak driving amplitude $A_0=0.1A_T$ (top) and strong driving amplitude $A_0=10A_T$ (bottom). The angular driving frequency is $\Omega=0.1$ in Figs. 1–11.

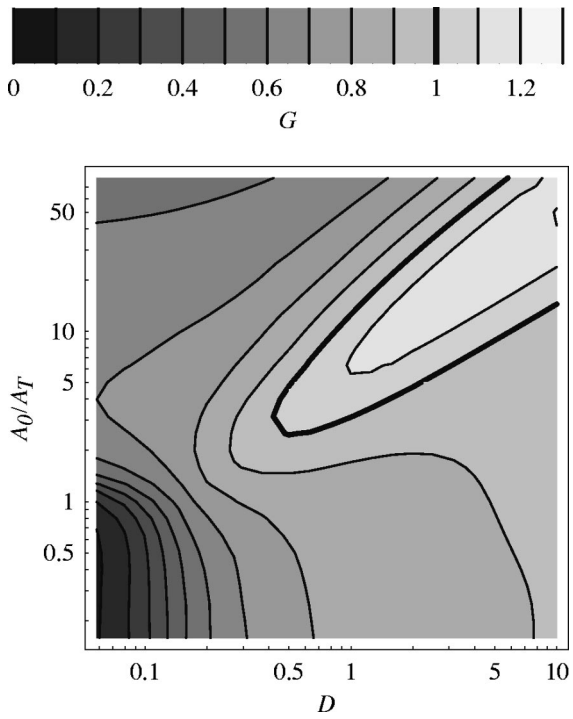

FIG. 2. Contour plot of the SNR gain G in (1) for the conventional SR setup in (2) versus noise intensity D and relative signal amplitude A_0/A_T. The gain is minimal near and below threshold driving and weak noise $D\leqslant 0.1$; it exceeds unity only for strong suprathreshold driving signals.

low noise would require impractically long simulation times due to the exponential time required to escape a well or reach equilibrium, preventing us from observing the asymptotic long-time result (4). Thus, we have limited our simulations to $D>0.04$. In a simulation or experiment with D much below this value, one would see single-well (intrawell) behavior only.

The main result of the SNR gain is depicted with Fig. 2 for an angular driving frequency set at $\Omega=0.1$. The overall behavior of the SNR gain remains qualitatively robust for smaller driving frequencies (not shown). The thick solid line in this two-dimensional contour plot of the scaled driving ratio A_0/A_T and scaled dimensionless noise intensity D marks the separation line between a gain below unity and a gain above unity. Most importantly, we note that the gain does not exceed unity for subthreshold signals. Within the considered parameter range of driving strength and noise intensity the gain reaches a maximal value around 1.20 on the peninsula corresponding to large driving strengths and large noise intensities. This behavior occurs in a parameter regime wherein no SR behavior for strong suprathreshold signals occurs. In contrast, the SNR gain assumes minimal values $G\gtrsim 0.08$ at low noise and around threshold driving $A_0\approx A_T$ and below. The nonlinear gain above unity is thus controlled by the quartic nonlinearity in the bistable potential. The behavior of this nonlinear gain regime is contrasted with Fig. 3, which depicts the SNR gain behavior for a pure quartic well. This monostable x^4 potential does not exhibit SR; its gain reaches from a minimum near $G\approx 0.7$ to maximal values along a diagonal band increasing from $G\approx 1.24$ at high noise to $G\approx 1.29$ at low noise. Note that the peninsula in Fig. 2 with a gain exceeding unity is ruled by this very monostable nonlinearity.

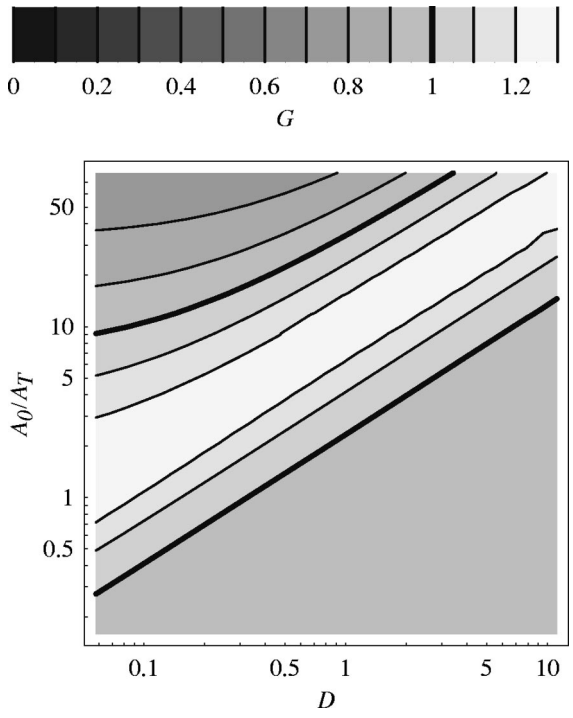

FIG. 3. Contour plot of the gain behavior versus noise intensity D and relative signal amplitude A_0/A_T in absence of bistability, i.e., the gain in a pure quartic well. In this case, both the spectral amplification and R_{out} are monotonically decreasing functions versus increasing noise intensity (no SR behavior). The regime of SNR gain exceeding unity for the bistable Duffing dynamics is clearly dominated by the quartic nonlinearity.

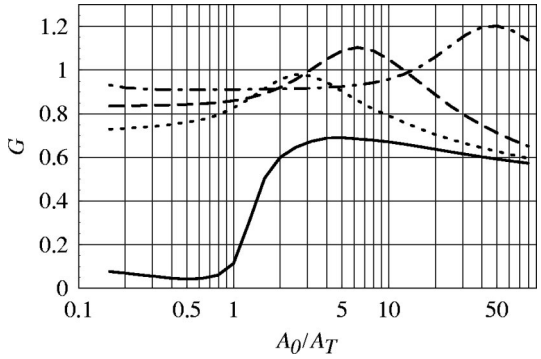

FIG. 4. The gain for the SR setup in Eq. (2) versus the relative signal amplitude A_0/A_T for four different noise intensities: $D=0.042\,88$ (solid line), $D=0.3678$ (dotted line), $D=0.9976$ (dashed line), and $D=9.976$ (dot-dashed line).

Some details of the gain behavior are made explicit with the cuts taken at fixed noise intensity (see Fig. 4) and fixed driving strength (see Fig. 5). The results in Fig. 4 depict the typical behavior of gain versus relative driving strength A_0/A_T at weak to small to moderate to large noise intensity. Generally, the gain behavior is distinctively nonmonotonic. A characterisitic feature is that for weak noise intensity the gain assumes a minimal value near and below threshold driving strengths. This situation is mirrored for the behavior of SNR gain versus noise intensity D in Fig. 5.

Next we shall elucidate in detail the nonlinear response behavior for the spectral amplification η and the regime of validity of linear response *per se*. The signal amplification η is shown in Fig. 6. We note that, for small driving strength, the spectral amplification exhibits the by now typical SR behavior. Interestingly enough, this SR behavior persists even for suprathreshold driving (note the dotted line in Fig. 6); the dynamical SR behavior (at $\Omega=0.1$) ceases to exist, however, for driving strengths exceeding roughly $A_0 \gtrsim 1.2A_T$, and decreases in amplitude for slower (adiabatic) driving (angular) frequencies, saturating around $A_0 \approx A_T$.

Of particular interest is the question of the regime of validity of linear response theory. We research this issue by computing, as a function of A_0, the ratio of full nonlinear SNR gain $G(A_0)$ to the SNR gain at a very small driving strength, $G_{LR}=G(0.1585A_T)$. The results are depicted in

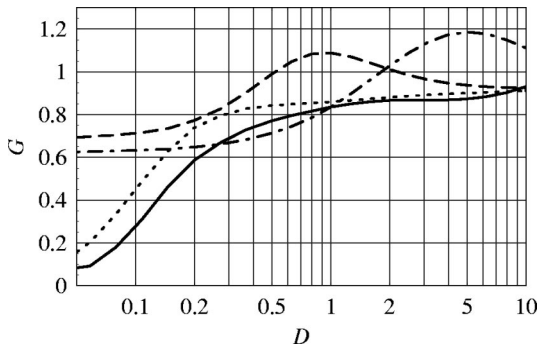

FIG. 5. Gain behavior for the white Gaussian noise driven, overdamped bistable Duffing dynamics versus noise intensity D at four different signal strengths: $A_0/A_T=0.1585$ (solid line), $A_0/A_T=1$ (dotted line), $A_0/A_T=5.012$ (dashed line), and $A_0/A_T=25.12$ (dot-dashed line).

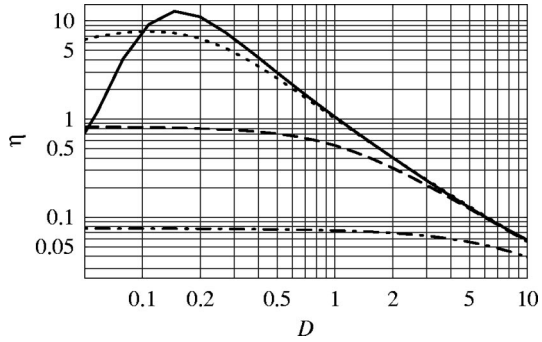

FIG. 6. Spectral amplification η versus noise intensity D for the SR setup in Eq. (2) for four different signal strengths: $A_0/A_T=0.1585$ (solid line), $A_0/A_T=1$ (dotted line), $A_0/A_T=5.012$ (dashed line), and $A_0/A_T=25.12$ (dot-dashed line). Note that the bell-shaped SR behavior still exists at the threshold driving $A_T \approx 0.3849$.

Fig. 7. For weak noise (solid curve), we find large deviations from the linear response prediction. This is so because the condition for linear response theory, namely, that the signal be weak compared to the noise intensity, is now violated. Note, however, that the regime of linear response at moderate to strong noise extends to large driving strengths well above threshold (see dashed and dot-dashed lines).

IV. ROLE OF NOISE COLOR

The case of white Gaussian noise presents an idealization which in many physical situations is not exactly realized. It is thus of importance to address the correction in the response to white noise, when the noise is colored. Several methods and approximations have been developed over recent years to investigate both numerically and analytically the role of finite noise correlation times, i.e., noise color; see Ref. [28] for a recent comprehensive review. For an overdamped dynamics driven by Gaussian, exponentially correlated noise—i.e., Ornstein-Uhlenbeck (OU) noise of constant intensity (thus possessing a proper white noise limit)—the increase of noise color (i.e., increasing the correlation time) tends to decrease the SR effect [3]. This result has repeatedly been demonstrated via analog simulations [29], analytical

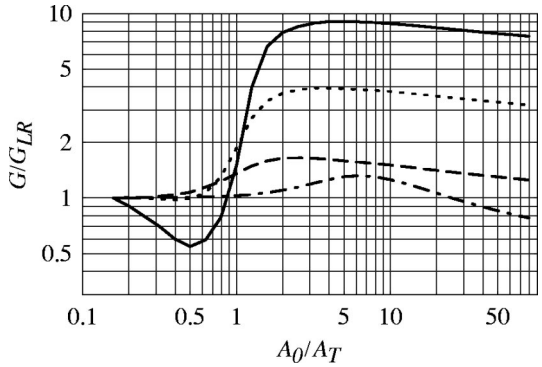

FIG. 7. Testing linear response: ratio of gain as a function of A_0 to gain at a fixed, small value of amplitude ($0.1585A_T$), for four different noise intensities: $D=0.04\,288$ (solid line), $D=0.079\,24$ (dotted line), $D=0.1464$ (dashed line), and $D=0.9976$ (dot-dashed line).

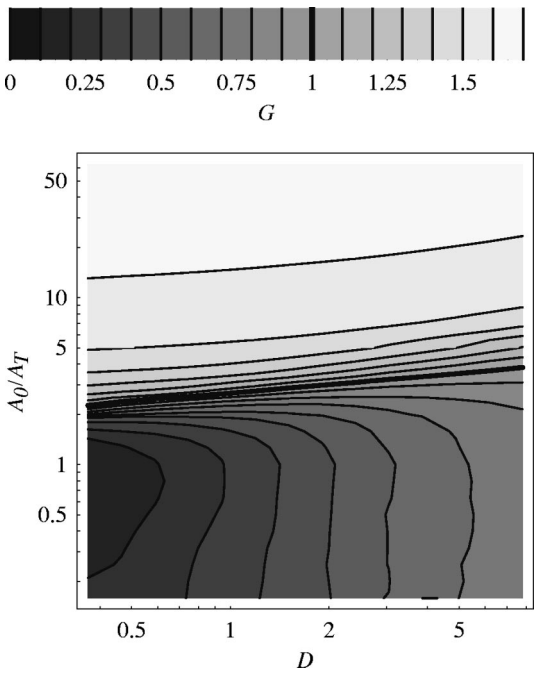

FIG. 8. Contour plot of the SNR gain for OU noise driven SR as a function of constant intensity D and relative signal amplitude A_0/A_T. The angular driving frequency is set at $\Omega=0.1$ and the noise correlation time is held fixed at $\tau_c=12.11$.

theory [30], experiments [31], and also by Monte Carlo simulations [32]. In contrast, inertial effects and certain other noise color characteristics can, in fact, also enhance the SR phenomenon [3,30,33]. Here, we shall focus on the SNR gain behavior when the dynamics is driven by Gaussian, exponentially correlated noise.

A. Gain for constant intensity OU noise

The corrections to the white noise limit are modeled by an OU noise $y(t)$ of constant intensity scaling. This implies an overdamped dynamics of the form

$$\dot{x}=x-x^3+A_0\cos(\Omega t+\phi)+y(t),$$
$$\dot{y}=-\frac{y}{\tau_c}+\frac{\sqrt{2D}}{\tau_c}\xi(t). \tag{11}$$

This OU noise $y(t)$ therefore possesses the following correlation:

$$\langle y(t)y(s)\rangle=\frac{D}{\tau_c}\exp(-|t-s|/\tau_c), \tag{12}$$

which does approach the case of white noise studied in the preceding section as $\tau_c\to 0$. The input power spectrum $\Xi(\omega)$ reads explicitly

$$\Xi(\omega)=\frac{2D}{1+\omega^2\tau_c^2}. \tag{13}$$

The gain behavior is depicted in Fig. 8 at a noise correlation time set at $\tau_c=12.11$. The role of strong noise color clearly has a dramatic effect on the overall behavior of the gain.

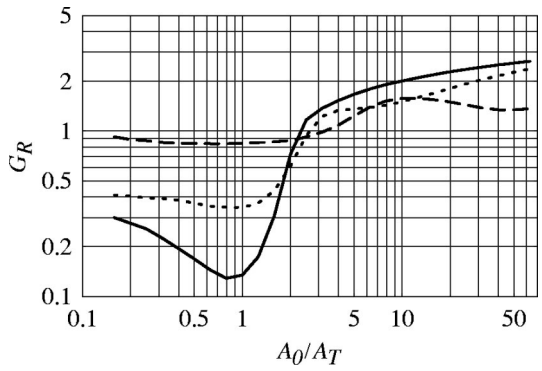

FIG. 9. Gain ratio G_R versus signal strength A_0/A_T between the gain taken at a noise color of $\tau_c=12.11$ (constant intensity scaling) and the gain taken at white noise $\tau_c=0$. Here $D=0.3678$ (solid line), $D=0.9976$ (dotted line), and $D=9.976$ (dashed line).

Most importantly, the separation line giving unity gain (note the thick line in Fig. 8) now extends down to very weak noise intensities D. The maximum in gain is also increased to a value $G\approx 1.62$. This enhancement of gain, however, does not occur uniformly. Figure 9 depicts the ratio of the corresponding gain values at $\tau_c=12.11$ and the white noise case. The gain can both be enhanced and suppressed over the white noise case, depending on the intensity of noise D and the signal strength.

In Fig. 10 we plot SNR gain versus τ_c for several D values and $A_0=A_T$. With constant intensity scaling, SNR gain appears to decrease monotonically with τ_c. This is in clear contrast to the constant variance case discussed next.

B. Gain for constant variance OU noise

In this subsection we address the case of OU noise driven SNR gain with a different noise scaling for $y(t)$, namely, the case of OU noise of constant variance scaling: it reads

$$\dot{y}=-\frac{y}{\tau_c}+\frac{\sqrt{2D}}{\sqrt{\tau_c}}\xi(t), \tag{14}$$

yielding for the noise correlation the form

$$\langle y(t)y(s)\rangle=D\exp(-|t-s|/\tau_c), \tag{15}$$

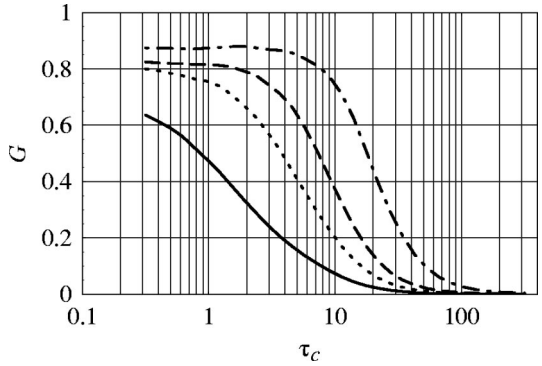

FIG. 10. Gain for OU noise driven SR with constant intensity scaling [see Eq. (12)] versus noise correlation time τ_c at different constant noise intensities D. Here $D=0.2$ (solid line), $D=0.5$ (dotted line), $D=1$ (dashed line), and $D=5$ (dot-dashed line). The signal strength is at threshold $A_0/A_T=1$.

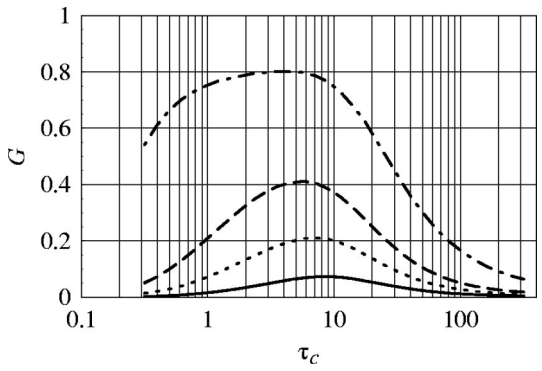

FIG. 11. Gain for OU noise driven SR with constant variance scaling [see Eq. (14)] versus noise correlation time τ_c at different constant noise intensities D. Here $D=0.02$ (solid line), $D=0.05$ (dotted line), $D=0.1$ (dashed line), and $D=0.5$ (dot-dashed line). The signal strength is at threshold $A_0/A_T=1$.

which approaches a vanishing white noise limit, i.e., $D\exp(-|t-s|/\tau_c)\to 2D\tau_c\delta(t-s)$ as $\tau_c\to 0$.

Although this situation formally consists of a mere substitution of the noise intensity of the form $D\to D\tau_c$, it implies different physics. For example, this scaling for OU noise has been shown to be capable of exhibiting resonance activation for the *escape rate* [34,35]; i.e., the rate exhibits a bell-shaped behavior versus increasing noise color. Since SR in the linear response limit is controlled by this very rate [3], we now expect a differing role of noise color for the spectral amplification and the SNR gain as well. Indeed, Fig. 11 exhibits the predicted bell-shaped, resonancelike (!) dependence of the SNR gain on τ_c, in contrast to the monotonically decreasing behavior seen with constant intensity scaling (Fig. 10).

V. GAIN FOR A ''NEURON'' MODEL

In this section we consider a model with a so-called ''soft'' potential. We again have a double-well potential, but in this case the potential grows as x^2 rather than x^4 for large x. For signal amplitudes and/or noise intensities that are large compared to the barrier height, we will essentially have motion in a parabola; i.e., we recover the linear response behavior.

The Langevin equation reads

$$C\dot{x}=-\frac{x}{R}+J\tanh(x)+A_0\cos(\Omega t+\phi)+\sqrt{2D}\xi(t). \tag{16}$$

Such a form can describe an (isolated) element of an electronic neural network, where x is the neuron's membrane potential, C is the input capacitance, R is the transmembrane resistance, and J is a self-coupling coefficient [36].

Figure 12 illustrates the SNR gain behavior for this model. As in the white noise driven Duffing model (2), the gain may exceed unity for suprathreshold driving only (note the island in Fig. 12 with $G\approx 1.19$). For very strong suprathreshold driving, however, the gain approaches unity. Under strong driving, the potential is dominated by its quadratic term, and we approach linear system behavior. The SNR gain, as we have defined it, must then necessarily approach unity.

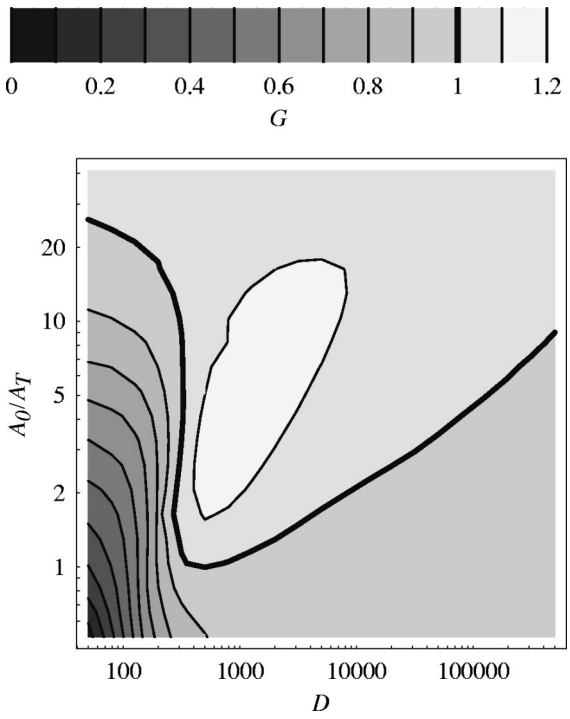

FIG. 12. Contour plot of the SNR gain G in Eq. (1) for the SR setup in Eq. (16) versus noise intensity D and relative signal amplitude A_0/A_T. The gain is minimal near and below threshold driving and weak noise $D\leqslant 50$; it exceeds unity only for suprathreshold driving signals. The gain at weak to moderate signal and noise is similar to the bistable Duffing oscillator in Eq. (2). In contrast, the suprathreshold gain behavior differs distinctly from the quartic double well: it saturates towards unity for strong suprathreshold driving. Other parameter values are $\Omega=1.225$, $C=1$, $R=0.018\,69$, and $J=216$. For these parameter values, the deterministic switching threshold is $A_T=116.6$.

VI. CONCLUSIONS AND OUTLOOK

In the present work we have concentrated on SNR gain, rather than other performance measures such as signal detection statistics or information-theoretic measures. For the archetypal SR setup we find—in contrast to the nondynamical threshold systems in [15–17]—that the SNR gain does not exceed unity for subthreshold signals. Moreover, the gain assumes rather small values for near-threshold or subthreshold driving strengths with weak noise. The gain does exhibit a very interesting feature as a function of increasing noise color: while this gain is monotonically decreasing for Ornstein-Uhlenbeck noise color of constant intensity scaling (thereby assuming a proper white noise limit), with increasing noise correlation time it does exhibit, in clear contrast, a resonancelike behavior for constant variance scaling. The latter feature reflects the resonant activation phenomenon [35] that occurs only for this form of Gaussian exponentially correlated noise. Generically, the SNR gain in these dynamical models of SR exceeds unity only for suprathreshold signals where the SR phenomenon in amplification and/or SNR is lost. Our results with suprathreshold sinusoidal driving refute

a recent conjecture that exceeding unity gain requires nonsinusoidal driving [15, third reference].

We remark that an output-input SNR gain exceeding unity does not necessarily imply, e.g., that the performance of an optimal detector on the SR system's output would exceed its performance on the input; however, the SNR does often correlate well with the performance of commonly used suboptimal detectors [9]. Furthermore, a high SNR is relevant in many applications *not* involving transduction of information through the SR system: e.g., generating a high-power, low-noise, monochromatic wave.

While the class of input signals considered in this work is amenable to the use of the SNR as an adequate measure of the system response, more complicated signals should, in general, have their responses characterized by more general measures, e.g., the mutual information or a distance measure of the ''separation'' of output probability densities in the presence and absence of the signal. The choice of measure is also predicated by the signal processing task at hand (detection or estimation, for instance); e.g., for detection, the minimum achievable probability of error can be expressed in terms of various information-theoretic distance measures (see, e.g., Robinson *et al.* [8]).

The construction of the ''optimal'' detector or filter for a given signal processing application might be a nontrivial task in general; however, it is at least clear that the SNR, as commonly defined in the SR literature, is *not* the optimal response measure for systems subject to complex signals. In fact, this SNR should be invoked only when the signal feature occurs primarily in a single narrow peak in the input or output power spectral density; this is usually the case *only* for a continuous time-sinusoidal input signal. The dramatic differences in SNR gain predicted, for example, by the ''generic'' systems discussed in this work and the threshold detectors subject to finite-width periodically separated input pulses [15,16] can, in fact, be attributed to the (somewhat questionable) choice of SNR as the measure characterizing the response in those works, where gains much higher than unity have been observed.

Stochastic resonance is a sophisticated effect that, cleverly applied to an *a priori* nonlinear device, can improve its response, particularly to a *subthreshold* signal in noise. For such input signals, a better response can generally be obtained by lowering the threshold (in this case, the potential barrier) between the stable states than by adding noise; however, threshold lowering may be difficult to achieve in some cases. This approach has been applied in some physical systems, most notably in systems characterized by static nonlinearities where the (in this case nondynamical) SR effect more closely resembles dithering [14,17]. Neural networks are thought to use the internal noise as a ''tuning'' parameter, cooperatively adjusting thresholds and internal parameters to achieve the best possible response, given the noise levels already present. A recent model [37] attempts to capture some of these features, notably ''adaptation,'' in an electronic ''fuzzy'' neural network that mimics a noisy nonlinear system whose dynamics are unknown. The fuzzy system tunes its ''if-then'' rules in response to samples from the response of the dynamical system and, effectively, learns the SR effect which it then uses to help itself converge to the dynamical system's characterization more rapidly. In networks, the response can also be enhanced by (linear or nonlinear) coupling through an array-enhanced stochastic resonance (AESR) effect [38]; the response will, of course, differ depending on whether the noise is uncorrelated from element to element or is instead ''global'' in character.

Stochastic resonance will *not*, however, improve the performance of an already optimal detector (e.g., an ideal matched filter—in this case, a single bin in the fast Fourier transform of the system output—for the detection of time-sinusoidal signals embedded in Gaussian noise); in the past, a failure to recognize this simple truth has led to a considerable amount of confusion in the literature. An exception [39] occurs when one considers a signal processing scenario with a nonlinear sensor connected to an optimal detector that is subject to a noise floor, e.g., from the ambience or the measurement and readout electronics, as happens quite often in practice. In this case noise added to the sensor or input signal *can*, in fact, enhance signal detectability, displaying a SR effect with the maximal response occurring for a value of the added noise intensity that depends on the noise floor. This is a result of the fact that the noise floor destroys the ''invertibility'' of the system or, alternatively viewed, renders an otherwise optimal detector suboptimal. Adding noise then helps overcome the noise floor via the amplification effect of SR.

ACKNOWLEDGMENTS

P.H. was supported in part by the German research foundation with the Sonderforschungsbereich SFB-486, Project No. A10. A.R.B., D.F., and M.E.I. acknowledge support from the Office of Naval Research through Grant No. N00014-99-1-0592 We acknowledge the Department of Defense High Performance Computing Modernization Program for computer time allocations on the NAVO and ERDC SGI/Cray T3E supercomputers.

APPENDIX: NUMERICAL TECHNIQUES

The general numerical method we use for solving a system of stochastic differential equations (SDE's) is the ''equivalent Heun scheme.'' Provided certain symmetry conditions hold, this scheme has a ''local'' (i.e., one-step) accuracy of $O(h^3)$, where h is the size of the time step and a ''global'' (arbitrary number of steps) accuracy of $O(h^2)$ [40]. If, as in our case, the noise term is independent of the system state (i.e., additive noise), then the aforementioned symmetry conditions are automatically satisfied; furthermore, the equivalent Heun scheme in this case reduces to the simpler Euler-Maruyama scheme.

The time step h must be chosen small enough to ensure numerical stability. This becomes an issue for large signal and/or noise, particularly in the Duffing case due to the presence of an x^3 term in the Langevin equation. For the Duffing and neuron simulations we used time steps of $h = 0.007\,670$ (8192 time steps per driving period) and 0.005 008 (1024 time steps per driving period), respectively.

We use the Box-Muller algorithm [41] to generate the required Gaussian random deviates (white Gaussian noise). To generate OU (colored) noise, we include in our system of

stochastic differential equations a white noise driven Ornstein-Uhlenbeck equation.

The numerically generated time series solutions must be windowed and Fourier transformed. The frequency resolution is inversely proportional to the window time length (i.e., the number of time series points per window), so it must be chosen large enough to provide sufficient frequency resolution around the driving frequency. We typically set the window length equal to 32 periods of the driving signal, resulting in a fundamental response exactly ''centered'' in the 33rd bin of the discrete Fourier transform (DFT) (the first bin is dc). Given our choices of h above, this implies 2^{18} points per Fourier transform for the Duffing simulations and 2^{15} for the neuron.

The window length should also be chosen long enough so that the simulation reaches equilibrium. In a double-well system with subthreshold driving, this puts a definite practical limit on the minimum value of the noise intensity D. For simulations involving colored noise, the window length should also be much greater than the noise correlation time.

Before performing the DFT, the data may be multiplied by a windowing function to help reduce ''leakage'' to neighboring bins of any strong, narrow peaks that do not fall precisely in the center of a frequency bin. However, in the models studied here, the peaks occur at the driving frequency and its multiples. By choosing the driving frequency to be centered in one of the frequency bins, we can eliminate leakage without using a windowing function.

We estimate the power spectrum by computing the average of the magnitude squared of the DFT's of many windows' worth of time series data (after discarding the first window's worth of data to skip over the start-up transient). We use the fast Fourier transform [41] to compute the DFT efficiently.

Typically we average 2048 windows' worth of data to allow us to estimate SNR's with errors of significantly less than 1 dB. Our contour plots are typically evaluated at 256 parameter space points. Such large computations necessitate using many processors in parallel. Each processor can be assigned the task of computing the result at one point in parameter space. Alternatively, all the processors can be given the task of computing the result at the same point in parameter space, but with less averaging and with each processor using a unique random number generator seed. The final result is then obtained by averaging over the results obtained by each processor. Current parallel supercomputers such as the Cray T3E, SGI Origin 2000, or IBM SP can compute one such contour plot in several hours' time if 64 processors are employed. Since very little interprocessor communication is required, networks of workstations may also be employed instead of supercomputers.

The values obtained for each frequency bin represent the power contained in that bin; i.e., they correspond to the integral of the power spectral density (PSD) over the width of the bin. We defined our SNR's (8) and (9) as signal power divided by the noise PSD. To obtain our numerical SNR estimate, note that the total power in the driving frequency bin equals the signal power plus noise power. We estimate the noise power in the driving frequency bin by considering the power in the nearby bins above and below the driving frequency bin (excluding bins very close to the driving frequency bin). We can either average them or fit a Lorentzian. We subtract this estimated noise power from the total power in the driving frequency bin to obtain the signal power. We divide the estimated noise power by the bin width to obtain an estimated noise PSD; the signal power is then divided by the so-obtained noise PSD to obtain an SNR that agrees with our definition.

[1] K. Wiesenfeld and F. Jaramillo, Chaos **8**, 539 (1998).

[2] A. Bulsara and L. Gammaitoni, Phys. Today **49** (3), 39 (1996).

[3] L. Gammaitoni, P. Hänggi, P. Jung, and F. Marchesoni, Rev. Mod. Phys. **70**, 223 (1998).

[4] P. Jung and P. Hänggi, Europhys. Lett. **8**, 505 (1989).

[5] P. Jung and P. Hänggi, Phys. Rev. A **44**, 8032 (1991).

[6] B. McNamara and K. Wiesenfeld, Phys. Rev. A **39**, 4854 (1989).

[7] K. Shannon, Bell Syst. Tech. J. **27**, 379 (1948); **27**, 623 (1948); A. Feinstein, *Foundations of Information Theory* (McGraw Hill, New York, 1958); A. Wherl, Rep. Math. Phys. **30**, 119 (1991); W. Ebeling, J. Freund, and F. Schweitzer, *Komplexe Strukturen: Entropie und Information* (B.G. Teubner, Stuttgart, 1998).

[8] J.J. Collins C.C. Chow, and T.T. Imhoff, Phys. Rev. E **52**, R3321 (1995); C. Heneghan, C.C. Chow, J.J. Collins, T.T. Imhoff, S.B. Lowen, and M.C. Teich, *ibid.* **54**, R 2228 (1996); M. Stemmler, Network **7**, 687 (1996); A.R. Bulsara and A. Zador, Phys. Rev. E **54**, R 2185 (1996); A. Neiman, B. Shulgin, V. Anishchenko, W. Ebeling, L. Schimansky-Geier, and J. Freund, Phys. Rev. Lett. **76**, 4299 (1996); J.E. Levin and J.P. Miller, Nature (London) **380**, 165 (1996); L. Schimansky-Geier, J.A. Freund, A.B. Neiman, and B. Shulgin, Int. J. Bifurcation Chaos Appl. Sci. Eng. **8**, 869 (1998); J.W.C. Robinson, D.E. Asraf, A.R. Bulsara, and M.E. Inchiosa, Phys. Rev. Lett. **81**, 2850 (1998); N.G. Stocks, *ibid.* **84**, 2310 (2000); I. Goychuk and P. Hänggi, Phys. Rev. E **61**, 4272 (2000).

[9] M.E. Inchiosa and A.R. Bulsara, Phys. Rev. E **58**, 115 (1998); **53**, 2021R (1996); M.E. Inchiosa, A.R. Bulsara, J.F. Lindner, B.K. Meadows, and W.L. Ditto, in *Chaotic, Fractal, and Nonlinear Signal Processing*, edited by R. A. Katz, AIP Conf. Proc. No. 375 (AIP, Woodbury, NY, 1996), pp. 401–419.

[10] C. Presilla, F. Marchesoni, and L. Gammaitoni, Phys. Rev. A **40**, 2105 (1989).

[11] M.I. Dykman, R. Mannella, P.V.E. McClintock, and N.G. Stocks, Phys. Rev. Lett. **65**, 48 (1990).

[12] G. Hu, H. Haken, and C.Z. Ning, Phys. Lett. A **172**, 21 (1992).

[13] M.I. Dykman, D.G. Luchinsky, R. Mannella, P.V.E. McClintock, N.D. Stein, and N.G. Stocks, Nuovo Cimento D **17**, 661 (1995) (see p. 676); A. Neiman, L. Schimansky-Geier, and F. Moss, Phys. Rev. E **56**, R9 (1997); A. Neiman, F. Moss, L. Schimansky-Geier, and W. Ebeling, in *Applied Nonlinear Dynamics and Stochastic Systems Near the Millennium*, edited by J.B. Kadtke and A. Bulsara, AIP Conf. Proc. No. 411 (AIP, New York, 1997) (see p. 152).

[14] L. Gammaitoni, Phys. Rev. E **52**, 4691 (1995); Phys. Lett. A **208**, 315 (1995).
[15] L. Kiss, in *Chaotic, Fractal, and Nonlinear Signal Processing* [9], pp. 382–395; K. Loerincz, Z. Gingl, and L.B. Kiss, Phys. Lett. A **224**, 63 (1996); Z. Gingl, R. Vajtai, and L. B. Kiss, Chaos Solitons Fractals **11**, 1929 (2000).
[16] F. Chapeau-Blondeau, Phys. Lett. A **232**, 41 (1997); F. Chapeau-Blondeau and X. Godivier, Phys. Rev. E **55**, 1478 (1997).
[17] M.E. Inchiosa, A.R. Bulsara, A.D. Hibbs, and B.R. Whitecotton, Phys. Rev. Lett. **80**, 1381 (1998).
[18] P. Jung and P. Hänggi, Z. Phys. B **90**, 255 (1993).
[19] J. Gómez-Ordoñez and M. Morillo, Phys. Rev. E **49**, 4919 (1994).
[20] V.A. Shneidman, P. Jung, and P. Hänggi, Phys. Rev. Lett. **72**, 2682 (1994); V.A. Shneidman, P. Jung, and P. Hänggi, Europhys. Lett. **26**, 571 (1994).
[21] L. Gammaitoni, F. Marchesoni, E. Menichella-Saetta, and S. Santucci, Phys. Rev. E **51**, R3799 (1995).
[22] N.G. Stocks, Nuovo Cimento D **17**, 925 (1995).
[23] F. Apostolico, L. Gammaitoni, F. Marchesoni, and S. Santucci, Phys. Rev. E **55**, 36 (1997).
[24] L. Gammaitoni, M. Löcher, A. Bulsara, P. Hänggi, J. Neff, K. Wiesenfeld, W. Ditto, and M.E. Inchiosa, Phys. Rev. Lett. **82**, 4574 (1999); M. Löcher, M. Inchiosa, J. Neff, A. Bulsara, K. Wiesenfeld, L. Gammaitoni, P. Hänggi, and W. Ditto, Phys. Rev. E **62**, 317 (2000).
[25] G.J. Schmid, diploma thesis, University of Augsburg, 1999 (unpublished).
[26] M.E. Inchiosa and A.R. Bulsara, Phys. Rev. E **52**, 327 (1995).
[27] See in Ref. [3], Eq. (4.4) and Eqs. (4.9)–(4.24).
[28] P. Hänggi and P. Jung, Adv. Chem. Phys. **89**, 239 (1995).
[29] L. Gammaitoni, E. Menichella-Saetta, S. Santucci, F. Marchesoni, and C. Presilla, Phys. Rev. A **40**, 2114 (1989).
[30] P. Hänggi, P. Jung, C. Zerbe, and F. Moss, J. Stat. Phys. **70**, 25 (1993).
[31] R.N. Mantegna and B. Spagnolo, Nuovo Cimento D **17**, 873 (1995).
[32] C. Berghaus, A. Hilgers, and J. Schnakenberg, Z. Phys. B **100**, 157 (1996).
[33] L. Alfonsi, L. Gammaitoni, S. Santucci, and A.R. Bulsara, Phys. Rev. E **62**, 299 (2000).
[34] P. Pechukas and P. Hänggi, Phys. Rev. Lett. **73**, 2772 (1994).
[35] For a review, see: P. Reimann and P. Hänggi, in *Stochastic Dynamics*, edited by L. Schimansky-Geier and T. Pöschel, Lecture Notes in Physics Vol. 484 (Springer, Berlin, 1997), pp. 127–139.
[36] See, e.g., D. Amit, *Modelling Brain Function* (Cambridge University Press, Cambridge, England, 1989); J.J. Hopfield, Proc. Natl. Acad. Sci. U.S.A. **81**, 3088 (1984).
[37] S. Mitaim and B. Kosko, Proc. IEEE **86**, 2152 (1998).
[38] See, e.g., M. Löcher, D. Cigna, E.R. Hunt, G.A. Johnson, F. Marchesoni, L. Gammaitoni, M.E. Inchiosa, and A.R. Bulsara, Chaos **8**, 604 (1998), and references therein.
[39] M.E. Inchiosa, J.W.C. Robinson, and A.R. Bulsara, Phys. Rev. Lett. **85**, 3369 (2000).
[40] T.C. Gard, *Introduction to Stochastic Differential Equations* (Marcel Dekker, New York, 1988).
[41] W.H. Press, B.P. Flannery, S.A. Teukolsky, and W.T. Vetterling, *Numerical Recipes* (Cambridge University Press, Cambridge, England, 1989).